MASS PROFILES OF X-RAY BRIGHT RELAXED GROUPS: METHODS AND SYSTEMATICS

FABIO GASTALDELLO

IASF-INAF MILANO & UC IRVINE

D. BUOTE UCI

P. HUMPHREY UCI

L. ZAPPACOSTA TRIESTE

J. BULLOCK UCI

W. MATHEWS UCSC

F. BRIGHENTI BOLOGNA

X-RAY MASS DETERMINATION

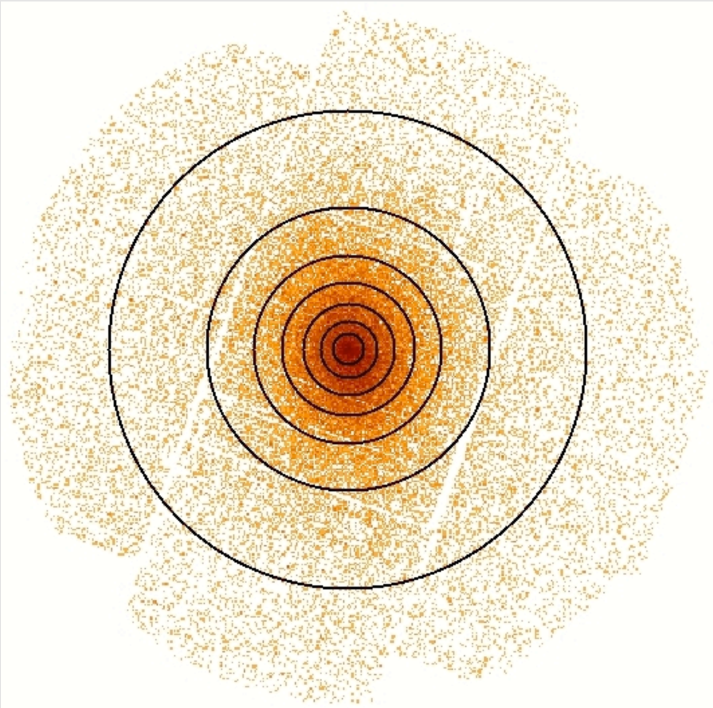

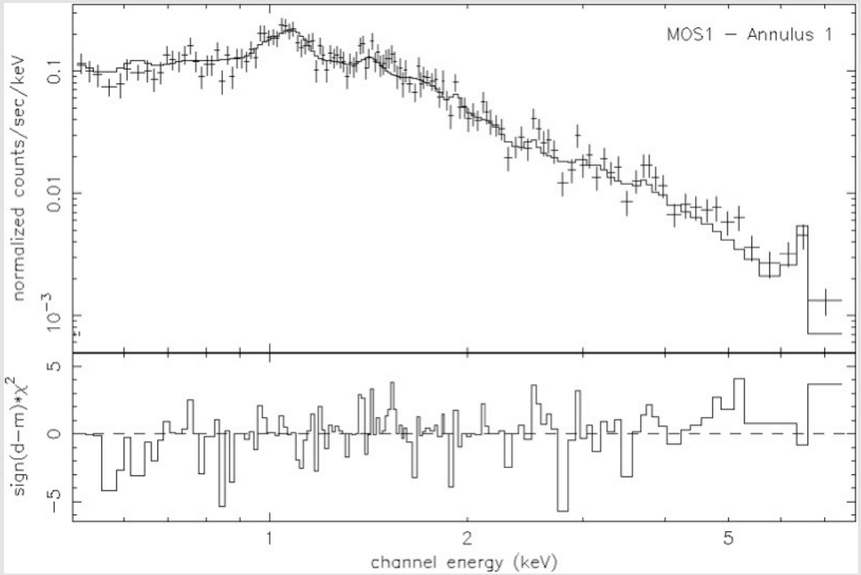

- Spectra averaged within circular annuli
- Normalization / shape of spectrum gives gas density / temperature

X-RAY MASS DETERMINATION

1. Assume spherical symmetry
2. Fit spectra with coronal plasma models and obtain (deprojected) spectral quantities
3. Fit parameterized functions to radial profiles of gas density and temperature
4. Assume hydrostatic equilibrium
5. Calculate the radial mass profile

$$M(<r) = \frac{r k_B T_g}{G \mu m_p}\left[-\frac{d \ln \rho_g}{d \ln r} - \frac{d \ln T_g}{d \ln r}\right]$$

DATA ANALYSYS

"Parametric mass method" is the principal approach of the study: we assume parameterizations for the temperature and mass profiles to calculate the gas density assuming HE

Gas density solution

$$\rho_g(r) = \rho_{g0}\frac{T_0}{T_g(r)}\exp\left(\frac{-\mu m_A G}{k_B}\int_{r_0}^{r}\frac{M\,dr}{r^2 T_g}\right)$$

We considered also the temperature solution

$$T_g(r) = T_0\frac{\rho_{g0}}{\rho_g(r)} - \frac{\mu m_A G}{k_B \rho_g(r)}\int_{r_0}^{r}\frac{\rho_g M\,dr}{r^2}$$

DATA ANALYSYS

$$\rho_g(r) = \rho_{g0}\frac{T_0}{T_g(r)}\exp\left(\frac{-\mu m_A G}{k_B}\int_{r_0}^{r}\frac{M\,dr}{r^2 T_g}\right)$$

•Fit gas density and temperature simultaneously assuming only parameterizations for temperature and mass.

Advantages:

- •better constraints on M
- •easy to interpret goodness of fit

X-RAY SYSTEMATICS

1. HYDROSTATIC EQUILIBRIUM
2. MULTIPHASE GAS/PROJECTION EFFECTS IN CORES
3. DISCRETE SOURCES IN Es
4. BKG SUBTRACTION
5. DEPROJECTION AND FITTING PROCEDURES

DATA ANALYSYS

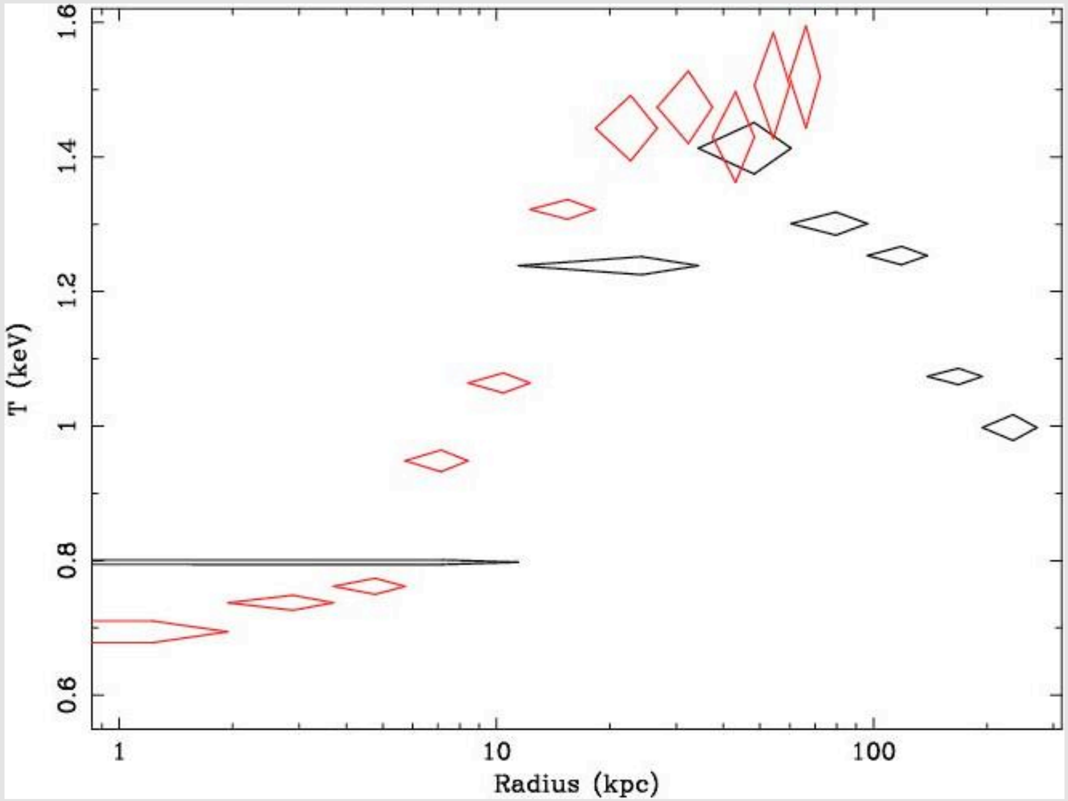

•Chandra inner regions

XMM outer regions

NGC 533

DATA ANALYSIS

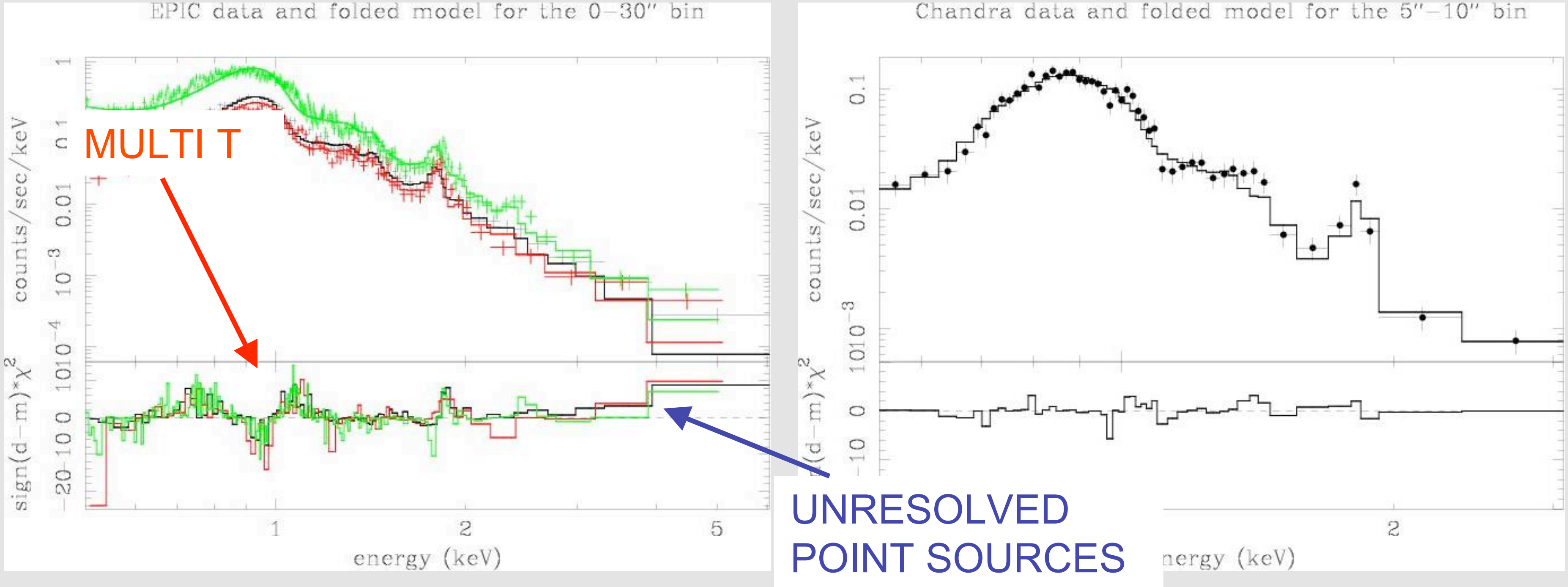

Chandra is crucial in the inner region where a steep temperature gradient is present

When data are available, we use Chandra in the core and XMM in the outer regions

DATA ANALYSIS

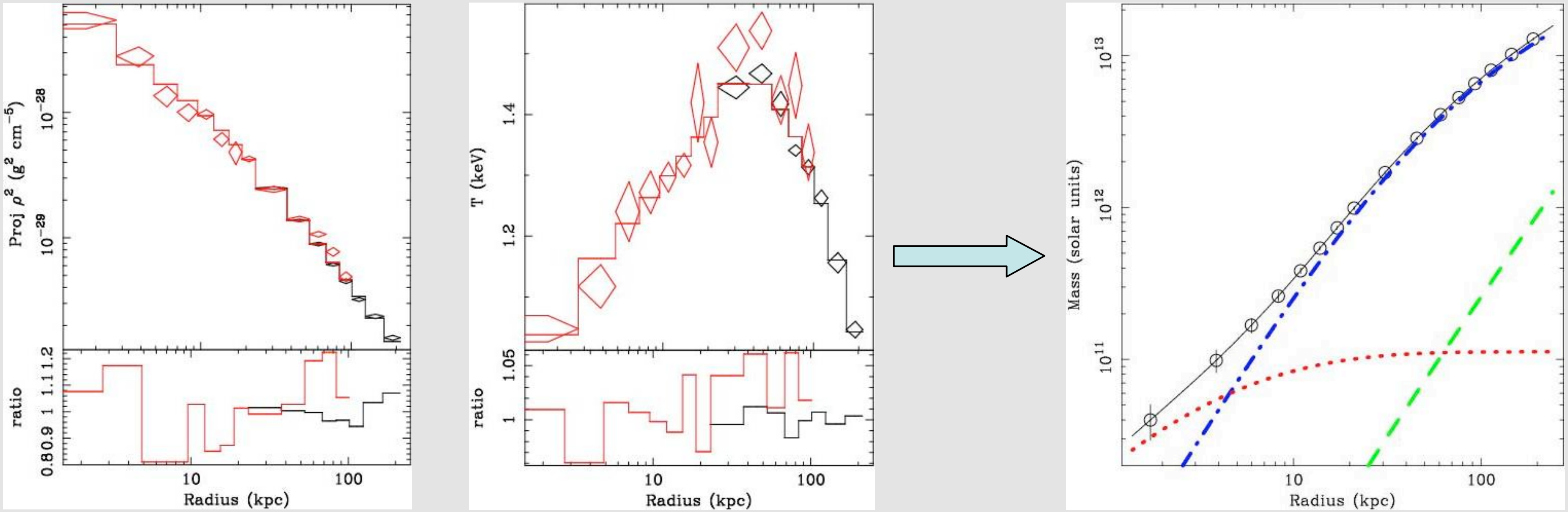

NGC 1550

- Projection of the 3D ρ and T thus obtained to the results from spectral analysis, including the radial variation of the plasma emissivity $\Lambda(T, Z_{Fe})$.

- Using an onion peeling deprojection (e.g., Fabian et al. 1981) gives consistent results with the above method

- Spectroscopic like T problem (e.g., Mazzotta et al. 2004). Folding

BKG SUBTRACTION

Bkg subtraction always crucial of course because of low surface brightness but different respect to clusters: particle background is not so crucial, important are the galactic components (and SWCX, we should routinely check for it, e.g. Carter & Sembay 08)

We completely model the various bkg components (e.g. Lumb et al. 2002), exploiting the fact that the source component, mainly characterized by the Fe-L shell, is clearly spectrally separated from the other bkg components

BKG MODELLING

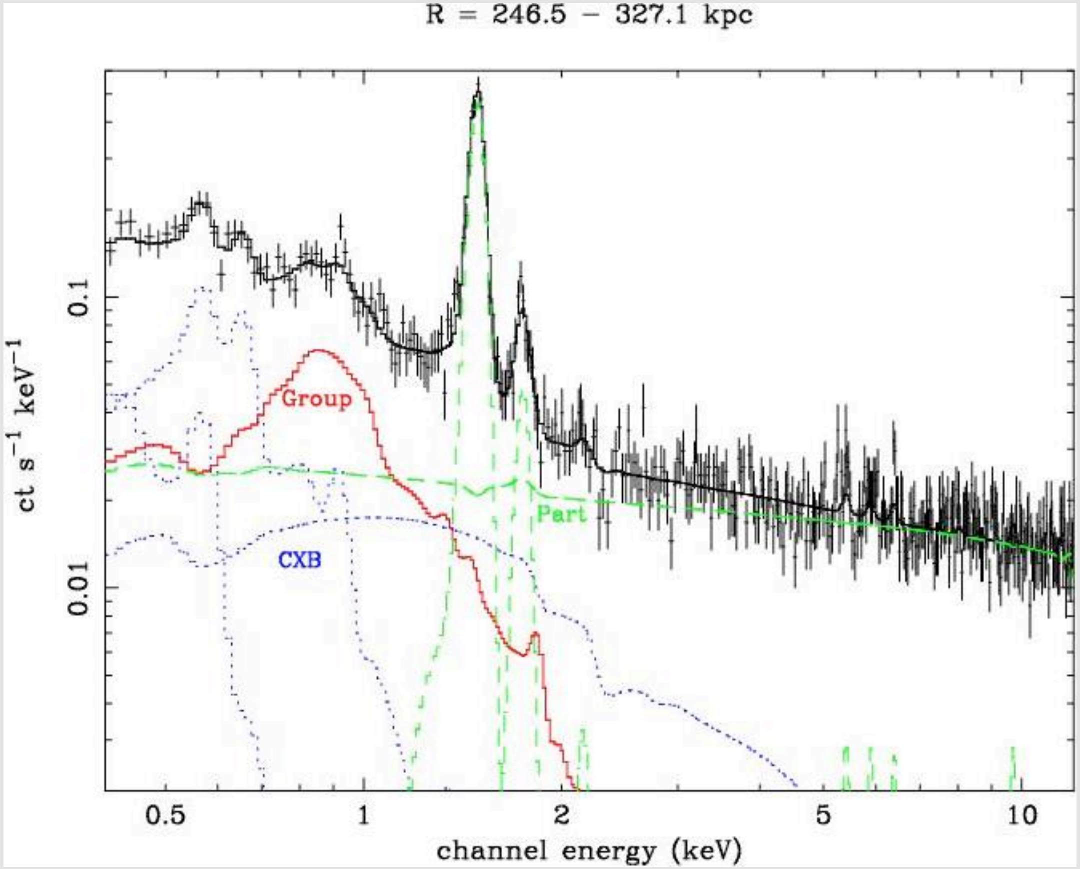

NGC 5044 offset

Buote et al. 2004

RESULTS

- After accounting for the mass of the hot gas, NFW + stars is the best fit model

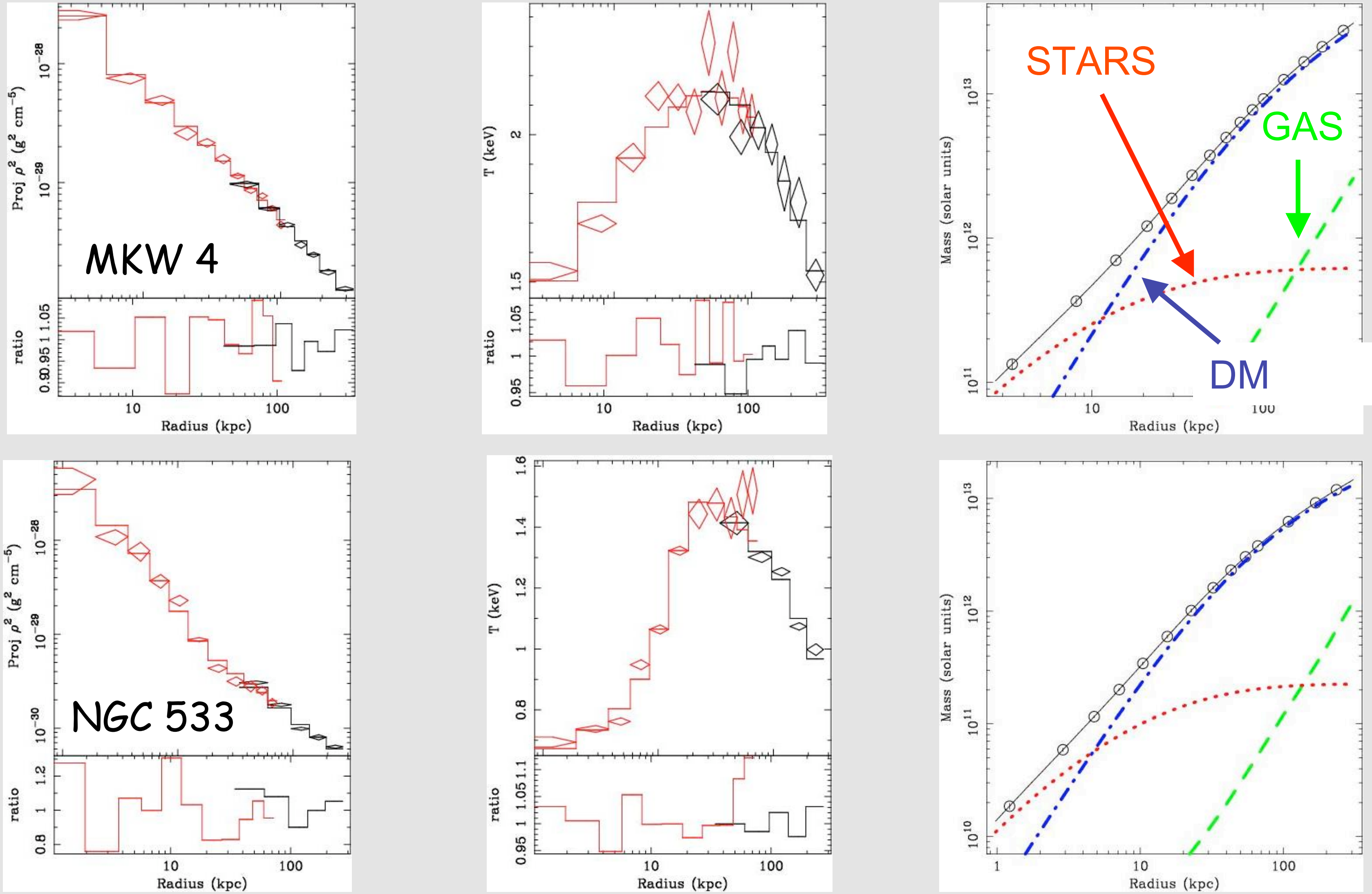

BKG MODELLING

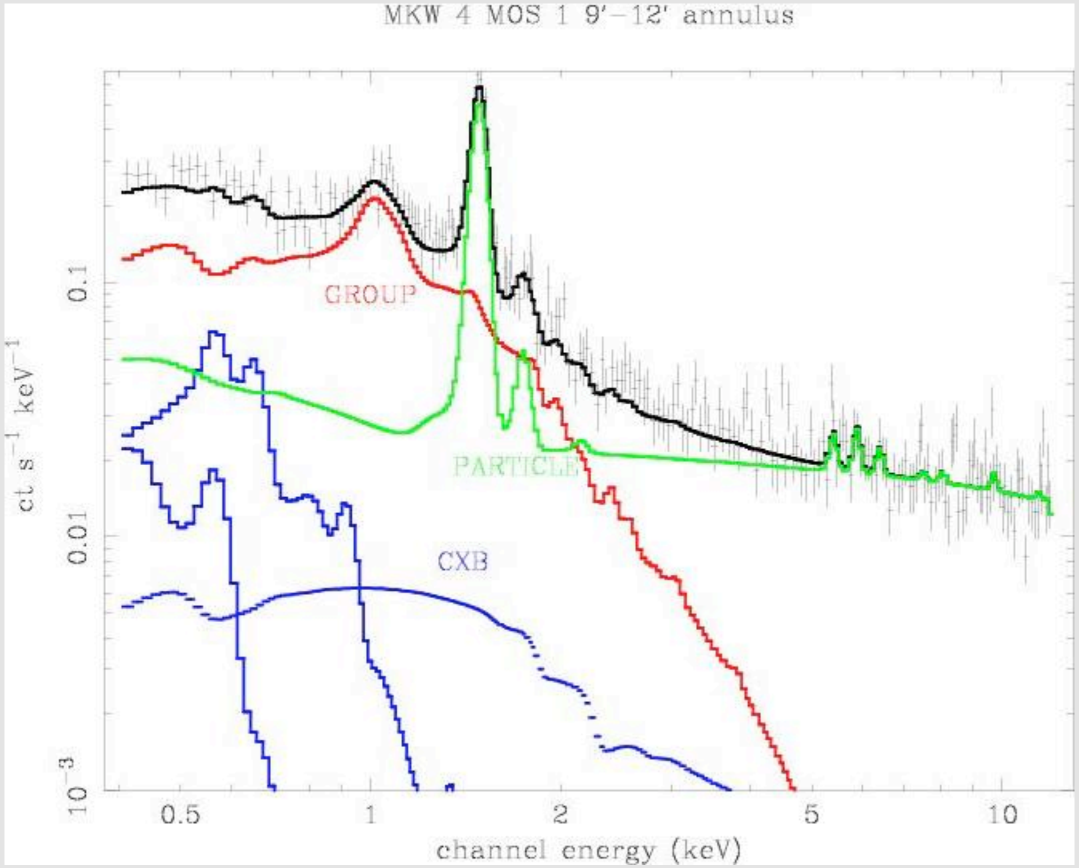

MKW 4

SELECTION OF THE SAMPLE

In Gastaldello et al. 2007 we selected a sample of 16 objects in the 1-3 keV range from the XMM and Chandra archives with the best available data with

•no obvious disturbance in surface brightness at large scale

•with a dominant elliptical galaxy at the center

•with a cool core

•with a Fe gradient

The best we can do to ensure hydrostatic equilibrium and recover mass from X-rays.

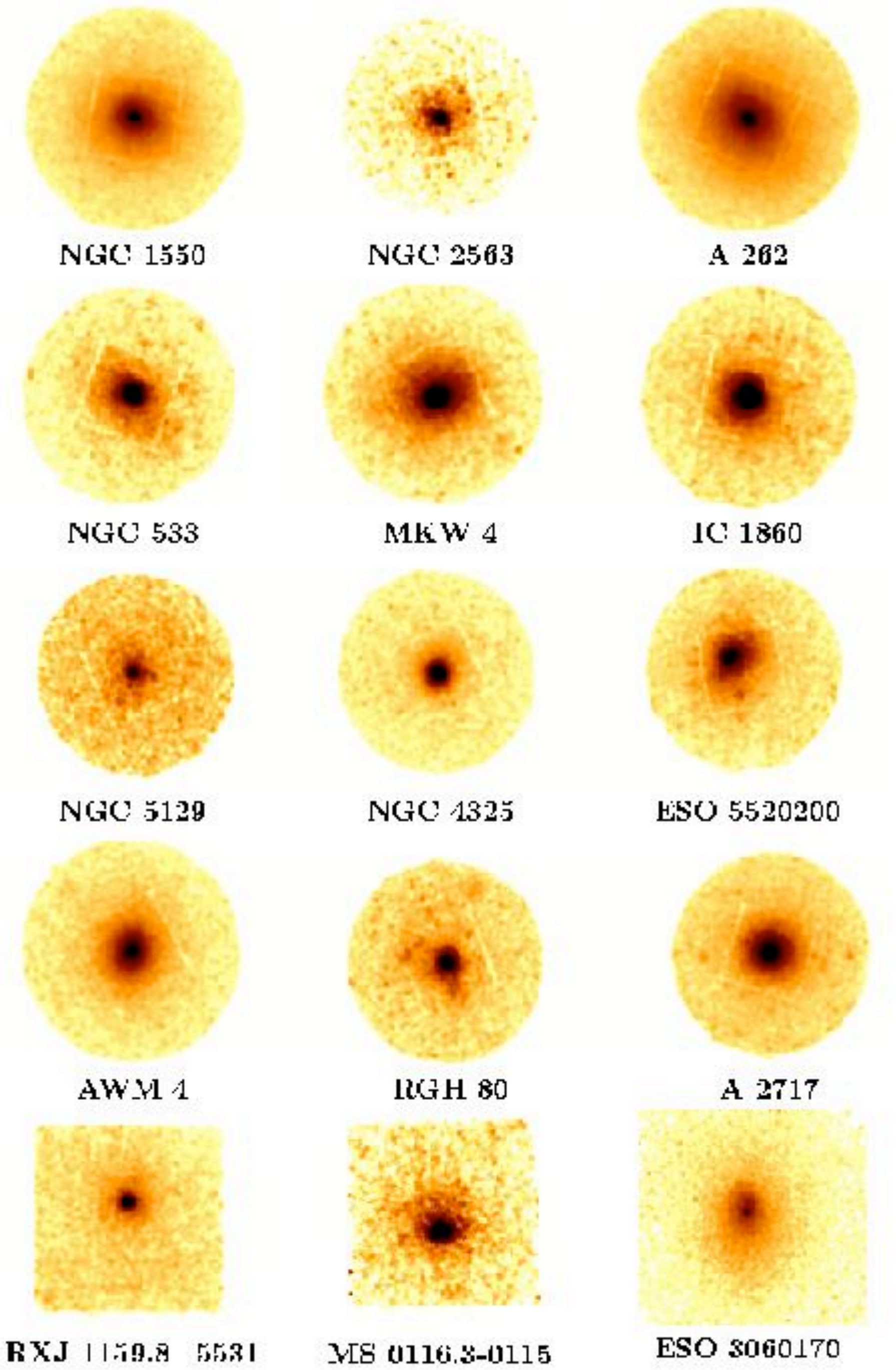

NGC 1550
NGC 2563
A 262
NGC 533
MKW 4
IC 1860
NGC 5129
NGC 4325
ESO 5520200
AWM 4
RGH 80
A 2717
RXJ 1159.8 5531
MS 0116.3-0115
ESO 3060170

The contribution of the stellar mass

Huge c > 30 in some previous X-ray studies (NGC 6482, Khosroshahi et al. 2004)

Baryons (stars) and DM different distributions

Fitting an NFW model to DM NFW + stellar component can bias high c

(Mamon & Lokas 2005)

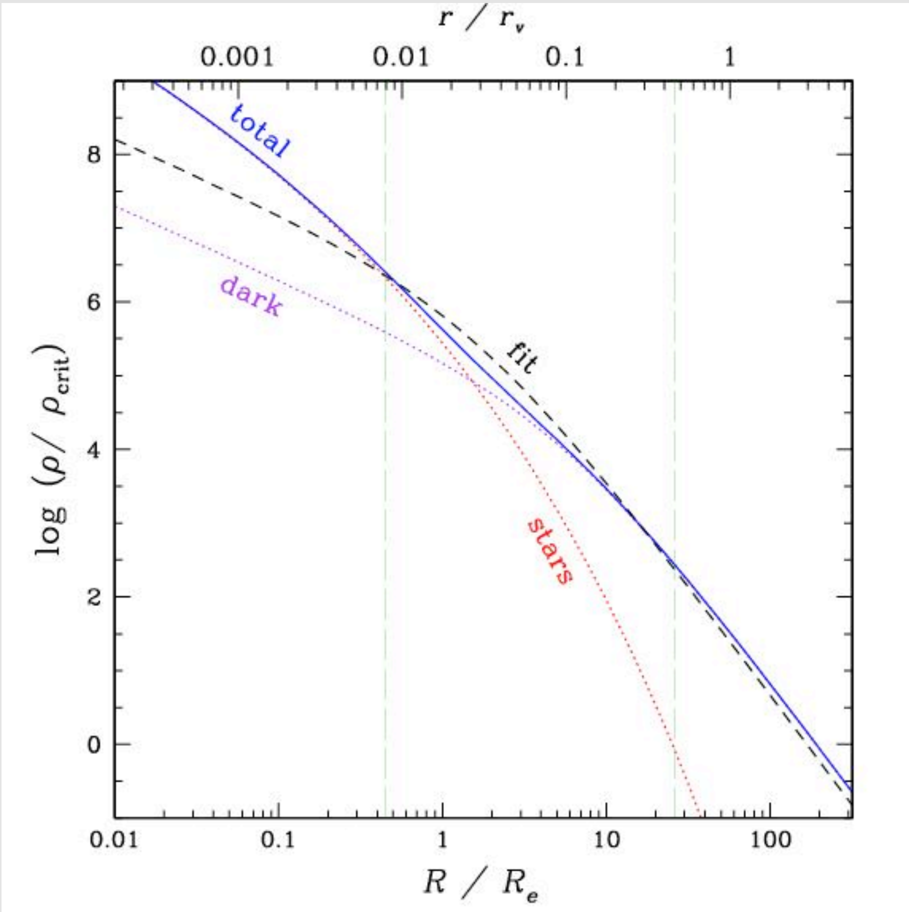

RESULTS

•No detection of stellar mass due to poor sampling in the inner 20 kpc or localized AGN disturbance

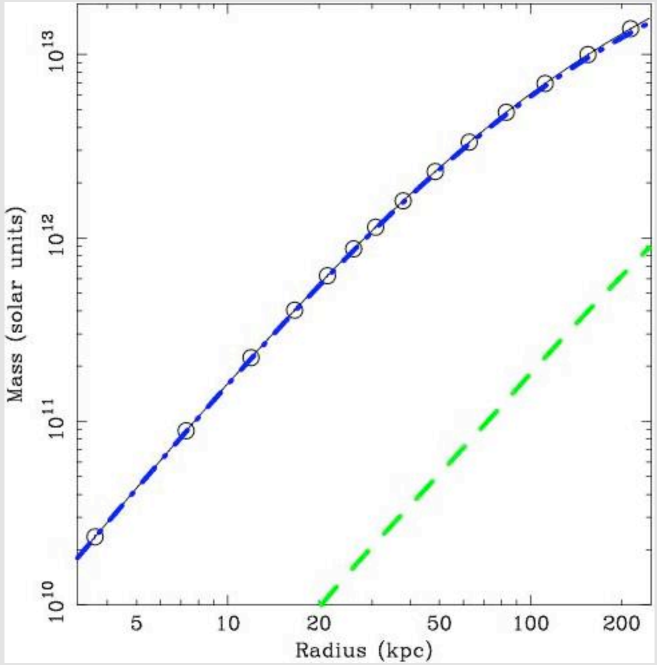

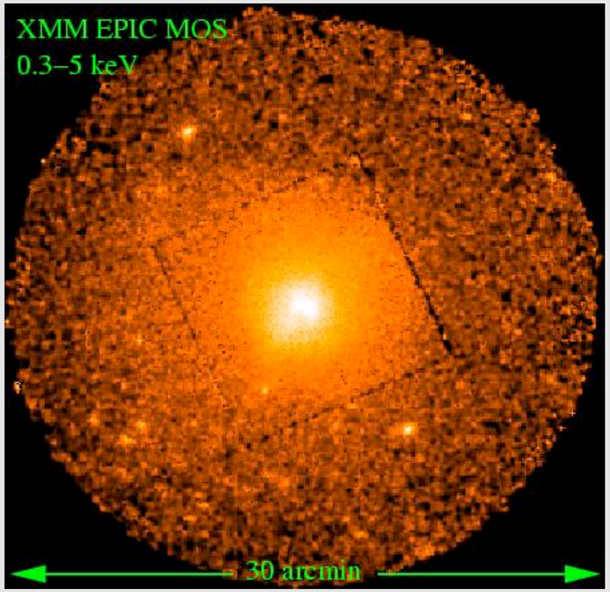

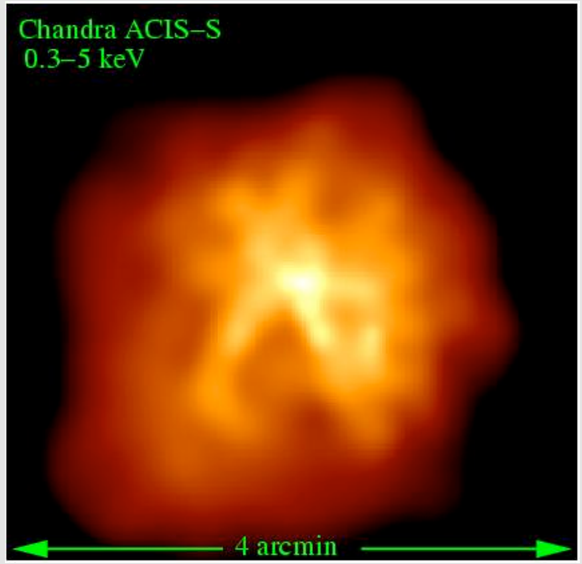

BUOTE+02

NGC 5044

GASTALDELLO+08

RESULTS

•No detection of stellar mass due to poor sampling in the inner 20 kpc or localized AGN disturbance

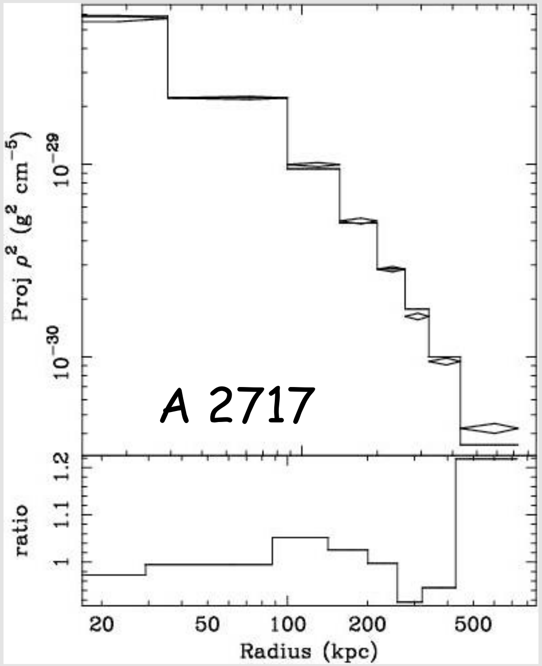

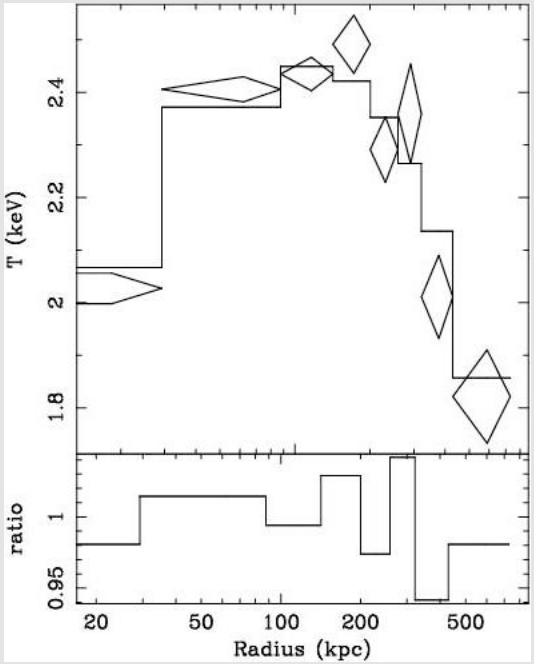

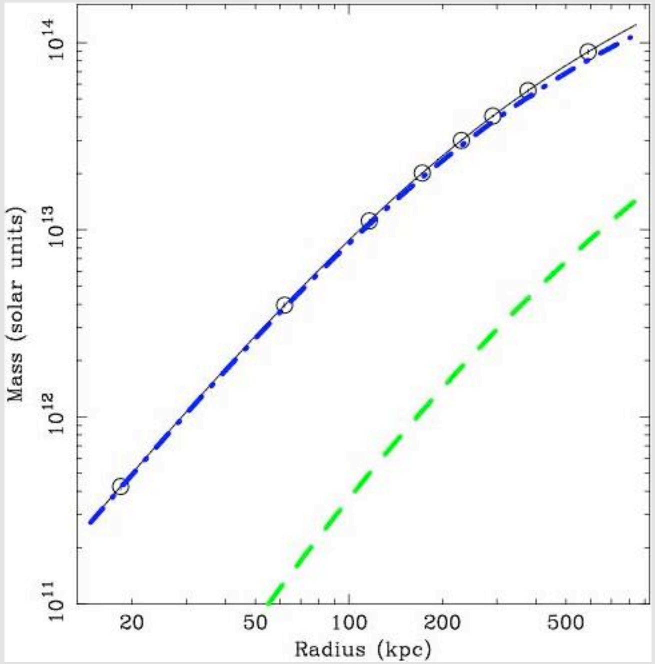

RADIAL RANGE

- RULE OF THUMB: SCALE RADIUS WELL IN THE MIDDLE OF THE FITTED RANGE (IS ENOUGH ?)
- IMPORTANT FOR GROUPS BECAUSE SCALE RADIUS IS SMALL. COMPARISON WITH SUN+08: FIXED INNER RADIUS OF FITTING RANGE OF 40 kpc. GOOD OVERALL AGREEMENT, SOME DISCREPANT CASES, THE HIGHER c ONES:
- NGC 1550 r_s 48 kpc c_{500} 9.0±0.6 SUN c_{500} 4.9±0.6

  NGC 533 r_s 43 kpc c_{500} 9.0±0.7 SUN c_{500} 4.6 +3.9 -2.3

SYSTEMATICS

TABLE 6

Systematic Error Budget

Group	Best Fit	ΔStatistical	ΔBackground	ΔSpectral	ΔMethod	ΔDeproj	Δr_e
			c_Δ				
NGC 5044	3.8	±0.1	−0.5	+0.2	+0.6	−0.3 (±0.2)	...
NGC 1550	4.5	±0.3	+0.4	±0.2	−0.1	−0.8 (±0.3)	+0.5
NGC 2563	2.4	±1.0	+2.6	+2.3	−0.1	+4.5 (±1.4)	...
A262	2.1	±0.2	+0.2	$^{+0.8}_{-0.6}$	−0.4	−0.4 (±0.2)	−0.2
NGC 533	6.1	±0.5	−1.7	−2.0	+1.1	−1.5 (±0.4)	+0.9
MKW 4	4.3	±0.3	−0.1	$^{+0.3}_{-0.7}$	−0.3	+0.8 (±0.7)	−0.3
IC 1860	3.2	±0.3	+0.1	$^{+0.9}_{-0.4}$	−1.3	...	...
NGC 5129	5.2	±0.9	+0.6	−0.4	−0.3	−0.2 (±2.2)	...
NGC 4325	2.8	±0.4	+0.7	+0.9	+0.3	−0.7 (±0.3)	...
ESO 5520200	2.5	±0.3	−0.2	−0.3	+0.1	+0.2 (±0.4)	...
AWM 4	3.0	±0.3	+0.1	−0.2	−0.1	−0.9 (±0.3)	...
ESO 3060170	2.1	±0.3	−0.4	$^{+0.8}_{-0.6}$	−0.3	−0.1 (±0.3)	...
RGH 80	5.1	±0.5	+2.1	+4.5	−2.6	+2.9 (±1.2)	...
MS 0116.3−0115	2.0	±0.8	+0.7	$^{+1.5}_{-0.5}$	+1.0	+2.3 (±1.9)	...
A2717	3.0	±0.2	+0.1	−0.2	−0.1	+0.6 (±0.3)	...
RX J1159.8+5531	5.6	±1.5	−0.9	+0.7	−1.2	+2.6 (±1.7)	...
			$M_\Delta/10^{13}\ M_\odot$				
NGC 5044	1.85	±0.04	+0.28	−0.10	−0.41	+0.34 (±0.09)	...
NGC 1550	1.42	±0.03	−0.04	−0.03	+0.02	+0.26 (±0.09)	+0.01
NGC 2563	0.92	±0.08	−0.06	−0.17	+0.01	−0.24 (±0.13)	...
A262	3.59	±0.14	−0.19	$^{+0.24}_{-0.62}$	+0.34	+1.00 (±0.31)	+0.10
NGC 533	1.30	±0.04	$^{+0.15}_{-0.01}$	+0.16	−0.04	−0.01 (±0.07)	−0.05
MKW 4	3.21	±0.10	−0.10	$^{+0.12}_{-0.07}$	+0.09	−0.86 (±0.18)	+0.03
IC 1860	2.36	±0.13	−0.08	$^{+0.12}_{-0.20}$	+0.65	...	...
NGC 5129	0.84	±0.07	$^{+0.08}_{-0.03}$	−0.02	...	−0.13 (±0.15)	...
NGC 4325	1.32	±0.16	−0.15	−0.20	−0.10	+0.53 (±0.45)	...
ESO 5520200	5.51	±0.51	+0.35	$^{+0.70}_{-0.13}$	−0.40	+0.49 (±0.71)	...
AWM 4	7.38	±0.61	−0.27	−0.70	+0.16	+2.01 (±0.87)	...
ESO 3060170	5.97	±1.14	+1.30	$^{+2.07}_{-0.74}$	+0.73	+0.68 (±1.37)	...
RGH 80	1.85	±0.07	$^{+0.26}_{-0.14}$	$^{+0.05}_{-0.40}$	+0.48	−0.07 (±0.19)	...
MS 0116.3−0115	4.92	±1.64	+0.46	$^{+0.68}_{-1.42}$	−1.12	−0.40 (±3.76)	...
A2717	10.68	±0.51	−0.03	+1.02	+0.49	−0.76 (±0.86)	...
RX J1159.8+5531	6.13	±3.30	+0.97	−0.29	+0.51	−1.87 (±0.72)	...
			$M_*/L_K\ (M_\odot\ L_\odot^{-1})$ (NFW+stars)				

IMPROVEMENTS

•GO TO LARGER RADII: XMM/SUZAKU OFFSET OBSERVATIONS

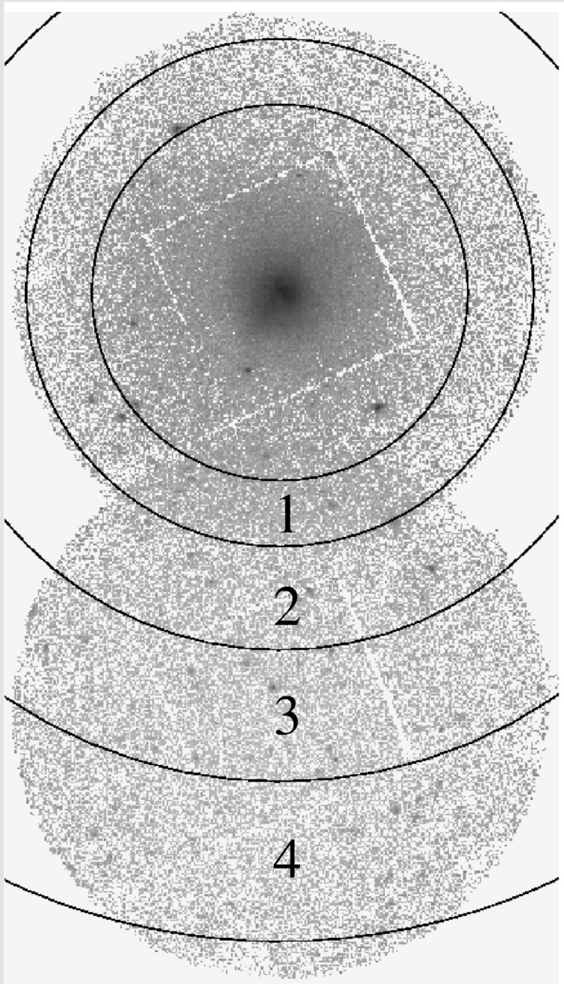

NGC 5044 offset

Buote et al. 2004

A SPECIAL ERA IN X-RAY ASTRONOMY

Chandra

XMM-Newton

- 1 arcsec resolution

- High sensitivity due to high effective area, i.e. more photons

DM DENSITY PROFILE

$$\rho(r) \propto r^{-1}(r_s + r)^{-2}$$

$$c = r_{vir} / r_s$$

The concentration parameter c do not depend strongly on the innermost data points, r < 0.05 r_{vir} (Bullock et al. 2001, B01; Dolag et al. 2004, D04).

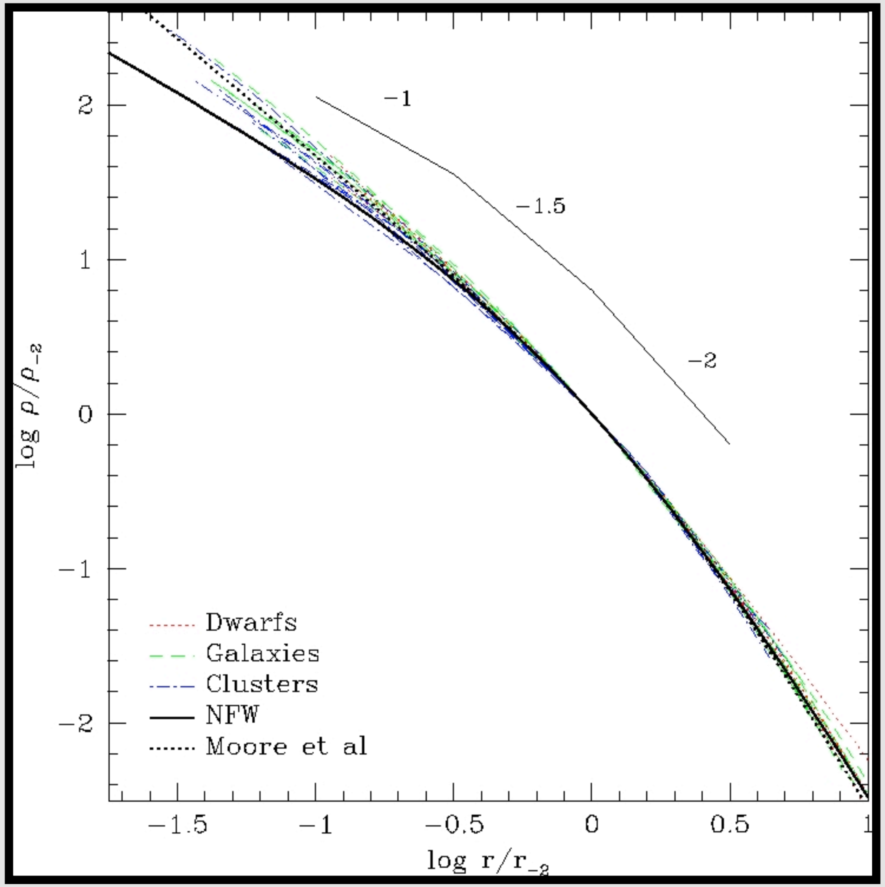

Navarro et al. 2004

Clusters X-ray results

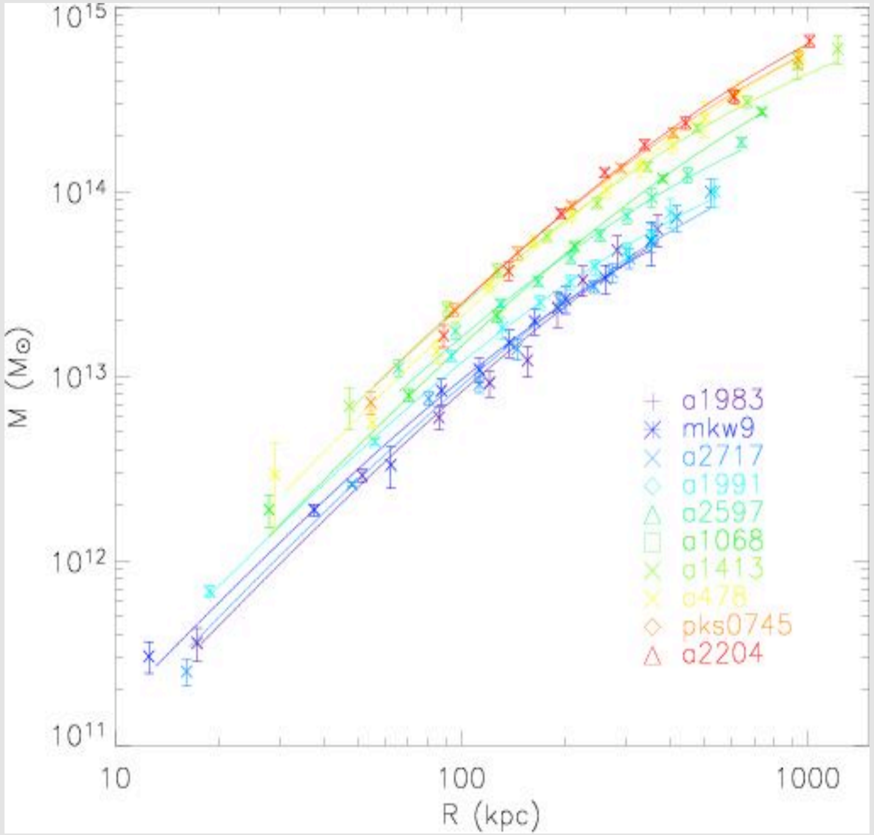

Pointecouteau et al. 2005

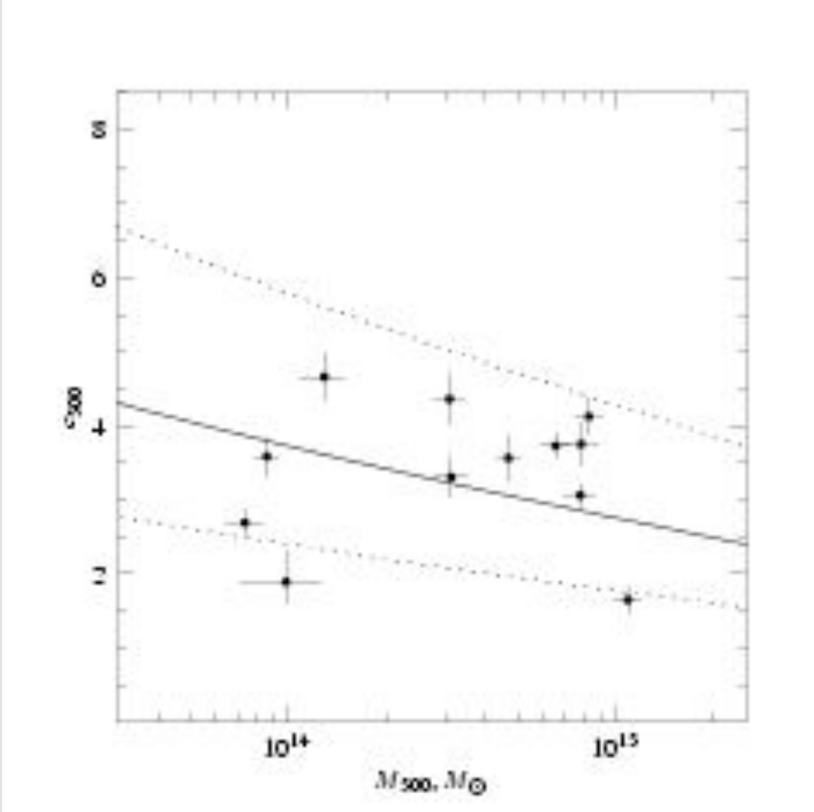

Vikhlinin et al. 2006

- NFW a good fit to the mass profile

- c-M relation is consistent with no variation in c and with the gentle decline with increasing M expected from CDM (α = -0.04±0.03, P05).

Table 1. The group sample and journal of observations

Group	z	Dist Mpc	ACIS Aim point	*Chandra* exp (ks)	EPIC filter	pn mode	*XMM* exp (ks)	r_{out}[c] kpc	Δ[d]
NGC 5044	0.0090	38.8	S	20.2	Thin	FF	19.5/19.3/8.9+ 38.4/38.4/32.0[b]	326	101.9
NGC 1550	0.0124	53.6	I	9.8 + 9.6[a]	Medium	FF	21.4/22.6/17.8	213	102.2
NGC 2563	0.0149	64.5			Medium	FF	20.4/20.8/16.5	219	102.4
A 262	0.0163	70.7	S	28.7	Thin	EFF	23.5/23.4/15.0	254	102.5
NGC 533	0.0185	80.3	S	36.7	Thin	FF	38.1/37.4/30.1	271	102.7
MKW 4	0.0200	87.0	S	29.8	Medium	EFF	14.0/13.9/9.4	336	103.1
IC 1860	0.0223	97.1			Thin	FF	34.1/34.8/28.0	323	103.1
NGC 5129	0.0230	100.2			Medium	FF	10.9/12.0/10.7	241	103.1
NGC 4325	0.0257	112.2	S	30.0	Thin	FF	20.8/20.8/14.7	238	103.3
ESO 5520200	0.0314	137.7			Thin	EFF	32.2/32.2/26.7	418	103.8
AWM 4	0.0317	139.0			Medium	EFF	17.5/17.2/12.5	455	103.9
ESO 3060170	0.0358	157.5	I	13.8 + 13.9[a]				245	104.2
RGH 80	0.0379	167.0	S	38.5	Thin	EFF	32.8/32.6/26.3	533	104.4
MS 0116.3-0115	0.0452	200.2	S	39.0				350	105.0
A 2717	0.049	217.7			Thin	FF	49.2/49.6/42.9	730	105.3
RXJ 1159.8+5531	0.081	368.0	S	75.0				625	108.0

Table 4. Results for the NFW virial quantities at selected overdensity

Group	Δ	r_s (kpc)	c_Δ	r_Δ (kpc)	M_Δ ($10^{13}\,M_\odot$)	$M_{gas,\Delta}$ ($10^{12}\,M_\odot$)	$f_{gas,\Delta}$	$M_{DM,\Delta}$ ($10^{13}\,M_\odot$)	$M_{*,\Delta}$ ($10^{10}\,M_\odot$)
NGC 5044	1250	77 ± 2	3.8 ± 0.1	295 ± 2	1.85 ± 0.04	1.21 ± 0.02	0.065 ± 0.001	1.72 ± 0.04	
NGC 1550	2500	48 ± 4	4.5 ± 0.3	215 ± 2	1.42 ± 0.03	1.02 ± 0.02	0.072 ± 0.001	1.31 ± 0.03	11.2 ± 4.1
NGC 2563	2500	76 ± 22	2.4 ± 1.0	185 ± 5	0.92 ± 0.08	0.31 ± 0.03	0.034 ± 0.001	0.89 ± 0.08	
Abell 262	2500	141 ± 16	2.1 ± 0.2	292 ± 4	3.59 ± 0.14	2.60 ± 0.08	0.072 ± 0.001	3.31 ± 0.13	22.1 ± 4.5
NGC 533	1250	43 ± 4	6.1 ± 0.5	262 ± 2	1.30 ± 0.04	0.87 ± 0.02	0.067 ± 0.001	1.19 ± 0.04	22.4 ± 2.2
MKW4	1250	81 ± 7	4.3 ± 0.3	353 ± 4	3.21 ± 0.10	2.84 ± 0.06	0.088 ± 0.002	2.87 ± 0.10	61.8 ± 7.2
IC 1860	1250	101 ± 12	3.2 ± 0.3	319 ± 6	2.36 ± 0.13	1.56 ± 0.05	0.066 ± 0.002	2.18 ± 0.12	26.4 ± 6.3
NGC 5129	1250	43 ± 10	5.2 ± 0.9	226 ± 7	0.84 ± 0.07	0.58 ± 0.06	0.069 ± 0.003	0.78 ± 0.07	$2.8^{+6.7}_{-2.8}$
NGC 4325	2500	75 ± 18	2.8 ± 0.4	208 ± 8	1.32 ± 0.16	0.66 ± 0.03	0.050 ± 0.004	1.26 ± 0.16	
ESO5526020	1250	171 ± 27	2.5 ± 0.3	422 ± 13	5.51 ± 0.51	3.35 ± 0.18	0.061 ± 0.002	5.17 ± 0.50	
AWM 4	1250	154 ± 17	3.0 ± 0.3	465 ± 13	7.38 ± 0.61	4.79 ± 0.29	0.065 ± 0.003	6.88 ± 0.59	$22.5^{+24.7}_{-22.5}$
ESO3060170	2500	162 ± 54	2.1 ± 0.3	343 ± 18	5.97 ± 1.14	3.45 ± 0.17	0.058 ± 0.005	5.62 ± 1.12	
RGH 80	500	78 ± 8	5.1 ± 0.5	397 ± 5	1.85 ± 0.07	2.85 ± 0.11	0.154 ± 0.003	1.56 ± 0.06	
MS 0116.3-0115	1250	202 ± 115	2.0 ± 0.8	405 ± 42	4.92 ± 1.64	1.97 ± 0.19	0.040 ± 0.009	4.73 ± 1.63	
Abell 2717	500	233 ± 18	3.0 ± 0.2	710 ± 11	10.68 ± 0.51	11.36 ± 0.29	0.106 ± 0.003	9.55 ± 0.49	
RXJ 1159.8+5531	500	104 ± 77	5.6 ± 1.5	584 ± 73	6.13 ± 3.30	5.10 ± 0.41	0.083 ± 0.019	5.57 ± 3.32	56.9 ± 10.5

Note. — Results for the mass profile fits. Δ refers to the overdensity chosen for the object, as the closest to the outer radius of the data. r_s is the scale radius of the NFW profile.

Name	Group	r_e (B) kpc (arcsec)	r_e (K) kpc (arcsec)	L_B 10^{10} $L_\odot$	L_K 10^{11} $L_\odot$
NGC 5044	NGC 5044	....	4.53 (24.5)	6.98	2.87
NGC 1550	NGC 1550	6.45 (25.5)	3.05 (12.1)	4.33	2.09
NGC 2563	NGC 2563	5.89 (19.3)	3.73 (12.2)	3.84	2.66
NGC 708	A 262	25.60 (77.1)	10.16 (30.6)	3.84	4.12
NGC 533	NGC 533	16.92 (45.4)	9.22 (25.2)	12.4	6.14
NGC 4073	MKW 4	19.24 (47.5)	10.25 (25.3)	13.7	7.18
IC 1860	IC 1860	8.34 (18.5)	8.03 (17.8)	6.08	4.38
NGC 5129	NGC 5129	13.34 (28.7)	6.60 (14.2)	12.0	4.99
NGC 4325	NGC 4325	....	5.22 (10.1)	4.61	2.33
ESO 552-020	ESO5520200	....	15.7 (25.0)	15.6	8.19
NGC 6051	AWM 4	10.21 (16.1)	10.33 (16.3)	9.91	7.50
ESO 306-017	ESO3060170	....	18.51 (26.0)	18.5	6.95
MCG 6-29-77	RGH80	....	5.11 (6.8)	....	2.93
MCG 6-29-78	RGH80	....	6.23 (8.3)	4.21	2.39
UGC 842	MS 0116.3-0115	....	9.69 (10.9)	9.29	5.77
ESO 349-22	A 2717	....	15.53 (16.2)	9.20	5.42
2MASSX J11595215	RXJ 1159.8+5531	....	9.77 (6.4)	23.6	10.3

Table 5. Stellar mass-to-light ratios

Galaxy	$L_{\rm K}/L_{\rm B}$	Fitted $M_\star/L_{\rm K}$ ($M_\odot/L_\odot$)	
		NFW+H90	NFW*AC+H90
NGC 1550	4.8	0.53 ± 0.20	0.24 ± 0.01
NGC 708	10.7	0.54 ± 0.11	0.14 ± 0.10
NGC 533	4.9	0.36 ± 0.03	0.11 ± 0.01
NGC 4073	4.6	0.86 ± 0.10	0.33 ± 0.04
IC 1860	7.2	0.60 ± 0.14	0.26 ± 0.01
NGC 5129	4.1	$0.06^{+0.13}_{-0.06}$	0.05 ± 0.01
NGC 6051	7.6	$0.30^{+0.33}_{-0.30}$	0.18 ± 0.01
2MASSX J11595215	4.4	0.55 ± 0.10	0.40 ± 0.05